JACC Vol. 25, No. 6
May 1995:1436–44

EXPERIMENTAL STUDIES

Echocardiographic Fourier Phase and Amplitude Imaging for Quantification of Ischemic Regional Wall Asynergy: An Experimental Study Using Coronary Microembolization in Dogs

HELMUT F. KUECHERER, MD, WOLFGANG SCHOELS, MD, LARRY D. STERNS, MD, FRCP, KIRSTEN FREIGANG, MD, GASPAR-DA-SILVA KLEBER, MD, JOHANNES BRACHMANN, MD, WOLFGANG KUEBLER, MD, FACC

Heidelberg, Germany

Objectives. **This study investigated whether echocardiographic Fourier phase and amplitude imaging can be used to evaluate ischemia-related regional wall asynergy.**

Background. **Because myocardial ischemia delays the onset and peak of endocardial inward motion and reduces its magnitude, Fourier phase and amplitude analysis of two-dimensional echocardiograms may be used to evaluate regional wall motion abnormalities objectively by analyzing temporal sequence and magnitude of endocardial motion.**

Methods. **Digital cine loops of left ventricular long- and short-axis views were obtained in six anesthetized dogs at baseline and 1 to 30 min after coronary microembolization and were mathematically transformed using a first-harmonic Fourier algorithm to obtain phase angles and amplitudes of endocardial segments. Mean phase angles and amplitudes were compared with visual wall motion analysis based on a scoring system and quantitative analysis based on segmental fractional area shortening derived from planimetry.**

Results. **Microembolization delayed segmental phase angles by 47 ± 44° in mild to moderate hypokinesia (fractional shortening [mean ± SD] 41 ± 13%) and by 77 ± 63° in severe hypokinesia (fractional shortening 13 ± 5%) and reduced segmental amplitudes from 80 ± 36 gray level intensity at baseline to 53 ± 34 in segments developing mild to moderate hypokinesia, and from 93 ± 36 to 35 ± 28 gray level intensity in segments developing severe hypokinesia. Shifts in segmental phase angles correlated better with dynamic shifts in segmental fractional area shortening than did changes in wall motion score ($r = -0.65$ vs. $r = 0.52$, $p < 0.001$).**

Conclusions. **Echocardiographic Fourier phase imaging can be used to evaluate ischemia-related regional wall asynergy, displaying contraction sequence and magnitude in a simple, objective format.**

(J Am Coll Cardiol 1995;25:1436–44)

Fourier phase and amplitude analysis of multigated equilibrium blood pool images has been used to evaluate regional wall motion (1–4). This method of "functional" or "parametric" imaging analyzes cyclic changes of left ventricular blood pools by fitting the time–activity curve of each picture element to a sinusoid function mathematically defined by its phase and amplitude. The resulting phase and amplitude images objectively display ventricular contraction sequence and magnitude. Ventricular contraction sequence can be derived from the phase image by measuring the sequence of color-encoded phase angles. Contraction magnitude can be derived from the amplitude image by measuring intensity-coded amplitudes. This method has also been applied successfully to cineventriculograms to analyze wall motion at rest and during exercise (5,6).

Recently, Fourier phase analysis of two-dimensional echocardiograms was used to localize accessory pathways in patients with the Wolff–Parkinson–White syndrome (7) by identifying the site of earliest endocardial inward motion during maximal pre-excitation.

Myocardial ischemia has been shown to reduce myocardial thickening, to delay the onset and peak of endocardial inward motion and to reduce its magnitude (9–12). Thus, Fourier phase and amplitude imaging should detect ischemia-induced regional wall motion abnormalities by identifying altered temporal sequence and magnitude of endocardial motion. To test this hypothesis, Fourier phase and amplitude analysis was applied to two-dimensional echocardiograms during coronary microembolizations in dogs.

From the University of Heidelberg, Internal Medicine III, Department of Cardiology, Heidelberg, Germany. This study was presented in part at the 43rd Annual Meeting of the American College of Cardiology, March 1994, Atlanta, Georgia. It was supported in part by the Deutsche Forschungsgemeinschaft, Bonn within the Sonderforschungsbereich 320. Dr. Sterns was the recipient of a Heart and Stroke Foundation of British Columbia and Yukon clinical fellowship (July 1992 through June 1993), Canada. Dr. Kleber, fellow of the Brazilian Society of Cardiology, was supported in part by the Brazilian Health Ministry, Brasilia under the Brazil–Germany Scientific Exchange Program.

Manuscript received July 19, 1994; revised manuscript received December 9, 1994, accepted December 15, 1994.

Address for correspondence: Dr. Helmut F. Kuecherer, University of Heidelberg, Department of Cardiology, Internal Medicine III, Bergheimer Strasse 58, 69115 Heidelberg, Germany.

0735-1097/95/$9.50
0735-1097(94)00554-4

Methods

Animal preparation. Studies were performed in six healthy mongrel dogs weighing 12 to 16 kg. The protocol was approved by the Committee on Animal Research of the University of Heidelberg. General anesthesia was introduced with Nembutal (pentobarbital 1.5 mg/kg body weight) injected through a forearm vein and maintained using nitrous oxide. Animals were placed on a temperature-regulated table, intubated and connected to a Harvard respirator pump for mechanical ventilation. The dogs were placed in a right lateral decubitus position, and the right groin was prepared for femoral arteriotomy under sterile conditions. A three-lead electrocardiogram (ECG) (I, II, aVL) was continuously monitored on a multichannel recording device (Electronics for Medicine).

Experimental protocol. Cardiac catheterization was performed through a right femoral arteriotomy. For baseline measurement of left ventricular pressures, a 5F pigtail catheter connected to a standard Statham transducer (P23dB) was positioned near the left ventricular apex under fluoroscopic guidance. Aortic pressures were then obtained by withdrawing the catheter into the ascending aorta. Subsequently, two-dimensional echocardiographic measurements of left ventricular short- and long-axis views were recorded on videotape. After completion of the baseline measurements, a 5F left coronary Judkins catheter was used for selective intubation of left anterior descending or left circumflex coronary artery. Coronary arteries were identified by hand injection of small amounts of contrast material (Soludrast) under fluoroscopy.

Coronary microembolization. Coronary embolizations were performed to induce myocardial ischemia and regional wall motion abnormalities using polystyrene latex microspheres (Polysciences), as described by Sabbah et al. (13). Microspheres were available in 5-ml vials containing deionized water and ~40,000 particles/ml solution. The particle diameter ranged from 77 to 102 μm. Microspheres were agitated by hand and injected as a bolus of 2 ml into respective branches of the left coronary artery. Hemodynamic and echocardiographic measurements were repeated 1, 5, 10, 20 and 30 min after injection.

Two-dimensional echocardiography. Two-dimensional echocardiography was performed using a commercially available sector scanner (Aloka, PPG Hellige, Stuttgart, Germany) and a 2.5-MHz transducer. Short- and long-axis cross-sectional views of the left ventricle were obtained from a low right parasternal transducer position with the animal in a right lateral decubitus position. Short-axis views were obtained at the level of the papillary muscle tips. Long-axis views were obtained by shifting the transducer slightly laterally and by rotating the transducer ~90° to yield an imaging plane perpendicular to the short-axis plane. Images were recorded on standard VHS videotape. Gain controls and brightness were adjusted individually in each dog and during each measurement period to allow adequate endocardial definition minimizing both endocardial dropout and background noise.

Digital processing. To allow transformation into a digital cine loop format, a single-lead ECG was displayed on the video screen of the ultrasound imaging system. Cross-sectional views were digitized from R to R wave using a conventional frame grabber board (RasterOps video color board 364P) at frame intervals of 33 ms. Images were stored on a commercially available Macintosh computer in a 350 to 400 × 450 to 500-image matrix for Fourier transformation (7).

Qualitative and quantitative analysis of regional wall motion. Regional wall motion was analyzed qualitatively by visual inspection of cine loops and quantitatively by manually tracing end-diastolic and end-systolic endocardial borders to calculate fractional area shortening. Visual assessment and planimetric measurements were performed by two independent observers uninformed of the phase images. Wall motion was visually graded and scored as follows: 3 = normal wall motion; 2 = mild to moderate hypokinesia; 1 = severe hypokinesia; 0 = akinesia; and −1 = dyskinesia. For quantitative analysis of regional wall motion, end-diastolic and end-systolic cross-sectional images were digitized using a commercially available computerized work station (Echo Com, PPG Hellige). The endocardial border was traced manually at its interface to the left ventricular cavity. Short- and long-axis views were divided into six defined wall segments according to American Society of Echocardiography guidelines (14). Segmental fractional area shortening was calculated using a customized wall motion analysis program (Echo Com, PPG Hellige). Regional wall motion analysis was based on a fixed-axis reference system (15). The mean value three consecutive cardiac cycles was calculated for each segment.

To assess the accuracy of visual analysis in detecting directional wall motion abnormalities, changes in segmental scores were compared with changes in measured segmental fractional area shortening.

Fourier phase and amplitude imaging. Digital cine loops were mathematically transformed using a first harmonic Fourier algorithm and customized software (7). Because the endocardium forms a black/white interface with the left ventricular cavity, ventricular contraction and relaxation result in a periodic shift of the black/white interface, leading to periodic changes in gray level intensity of each individual picture element (*pixel*) related to the endocardial region. The Fourier transformation fits the time–intensity curve of each individual pixel to a sinusoid function, characterized by its amplitude and phase. Amplitude relates to pixel intensity, and phase relates to the onset of intensity change. The phase shift between the actual sinusoid function and a pure cosine function, as a reference function, is measured in degrees defining phase angles. Phase angles were automatically transformed into intensity variables and displayed in gray shades (0–255). The spectrum of gray levels was color encoded using a cyclic color scale, as previously described (7). The color phase image displays the temporal sequence of endocardial motion in a composite format. Applied to endocardial surfaces and chamber walls, the phase angle sequence relates to the sequence of endocardial motion.

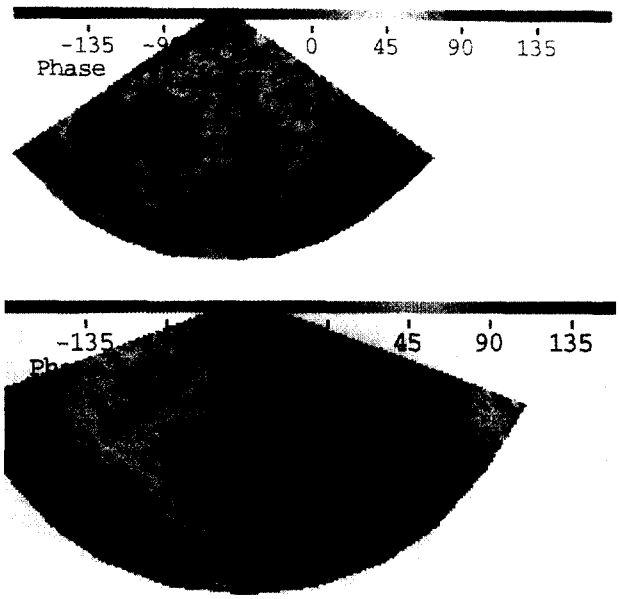

Figure 1. Normal long- (**top**) and short-axis (**bottom**) phase images. Normal regional wall motion is visualized by homogeneous color coding of phase angles within the endocardial regions (**green**), indicating synchronous endocardial motion.

By convention, we evaluated areas in relation to maximal endocardial inward motion. Because maximal endocardial inward motion occurs near the middle of the cardiac cycle, the fit of the time–intensity curve of pixels in these areas yields an inverted cosine curve. Therefore, by our convention, we expected normal wall motion to yield a phase angle near 180°. Because in radionuclide phase imaging normal motion is displayed in green color shades, we converted the color scale to yield green color shades for normal systolic endocardial motion (Fig. 1). Delayed endocardial inward motion (tardokinesia) was expected to shift the phase angle color code in focal endocardial regions. Hypokinesia was expected to delay phase angles. Akinesia was expected to result in a lack of intensity changes, yielding indefinite or indeterminate phase angles. Dyskinesia was expected to shift phase angles by ~180°, corresponding to its paradoxic wall motion pattern.

To quantitate regional phase angles objectively, histograms were obtained in defined ventricular wall segments, and mean segmental phase angle was calculated. To exclude presumed artifacts, a threshold was used to omit analysis of pixels with phase angles occurring less frequently than 5% of the histogram peak. The segment with the earliest phase angle in reference to the R wave was defined as the segment contracting earliest (relative phase angle of 0°). The phase angle delay of each segment to the reference segment was hence calculated. This "normalization" procedure allows comparison of different cross-sectional views and different ventricles.

Amplitude is color coded in shades of blue (low amplitude) and red (high amplitude), relating to the magnitude of intensity changes. Normal, homogeneous endocardial motion was expected to yield uniform amplitudes, equally distributed around the endocardial region. Hypokinesia (reduced extent of endocardial motion) was expected to result in low amplitudes, whereas akinesia was expected to result in a lack of regional amplitudes. In dyskinetic segments, amplitudes were expected to indicate outward motion. Amplitudes were measured using thresholding to determine the intensity at which ~50% of the image pixels in the regions of interest were still visualized as the threshold was gradually increased. With regard to endocardial motion, there is less intensity change of image pixels within a constant region of interest when the extent of motion is reduced, resulting in a reduction in overall amplitudes.

In vitro model of temporal sequence of endocardial motion. To test whether the first harmonic Fourier algorithm applied to two-dimensional echocardiography correctly detects temporal shifts of endocardial motion, a phantom model mimicking ventricular contraction was designed. In brief, a water-filled latex balloon (volume 170 ml) shaped like an ellipse of revolution was positioned in a water bath, and echocardiographic short-axis cross sections were recorded on videotape. Serial short-axis views, in a sequential hierarchy of size, were digitized in a cine loop format to yield an analog model of periodic endocardial motion. For the purpose of this study, the timing of the "end-systolic" frame (smallest cross section) was varied to mimic delayed endocardial inward motion while keeping the fundamental frequency of periodic motion constant, thus varying the relative durations of systole and diastole. Phase histograms were obtained from six segments along the balloon wall circumference corresponding to the end-systolic position of the ventricular endocardium, to obtain mean phase angles. The phase angles derived from the "end-systolic" frame were correlated with the temporal delay obtained from frame-by-frame analysis.

Comparison of phase angle shifts with temporal sequence of endocardial motion assessed by M-mode echocardiography in normal humans. To test whether the phase angle sequence derived from Fourier phase analysis of two-dimensional cine loops correctly identifies the temporal sequence of wall motion, we compared phase angles of endocardial motion in septal and posterior wall regions with the temporal sequence of motion derived from M-mode echocardiograms in six normal healthy male subjects, 25 to 36 years old, undergoing transthoracic echocardiography. The time to peak septal and posterior wall motion was measured as the time from peak R wave to maximal endocardial excursion of the septal and posterior walls.

Statistical analysis. Analysis of variance for multiple repeated measurements was used for comparison of two-dimensional echocardiographic variables and phase and amplitude variables between measurement periods. To compare directional changes in segmental fractional area shortening with directional changes in phase angles and amplitudes, we used linear regression analysis. Results are presented as mean value ± 1 SD.

Results

Cardiac hemodynamic variables. Coronary microembolization increased left ventricular end-diastolic and end-systolic

Table 1. Two-Dimensional Echocardiographic and Hemodynamic Variables

	Four-Chamber View			Short-Axis View				
Period	EDV (ml)	ESV (ml)	EF (%)	Diastolic CSA (cm^2)	Systolic CSA (cm^2)	FS CSA (%)	Heart Rate (beats/min)	LV Pressure (mm Hg)
Control								
Mean	28.1	8.6	71.4	8.4	2.8	67.0	165.0	107.0
SD	7.9	5.4	9.2	1.9	0.9	7.2	9.0	20.6
1 min								
Mean	34.6*	23.7*	38.7*	11.1*	8.3*	27.5*	153.0	106.0
SD	12.5	11.9	18.8	2.3	3.1	20.7	20.0	17.2
5 min								
Mean	35.3*	21.0*	40.8*	10.7*	7.1*	34.1*	161.0	99.0
SD	7.7	6.9	12.3	1.4	1.7	9.9	25.0	25.0
10 min								
Mean	30.0	17.5*	42.8*	10.8*	6.8*	39.0*	165.0	103.0
SD	8.2	6.5	12.1	1.8	2.0	12.5	25.0	28.0
20 min								
Mean	29.7	17.0*	44.2*	10.4*	6.9*	34.6*	161.0	110.0
SD	5.8	7.0	17.1	1.9	2.1	15.2	23.0	18.0
30 min								
Mean	26.2	14.6*	45.7*	10.7*	6.1*	44.2*	168.0	109.0
SD	5.9	6.2	14.0	1.8	2.1	12.0	21.0	16.2

*$p < 0.05$ versus control. CSA = cross-sectional area; EDV = end-diastolic volume; ESV = end-systolic volume; EF = ejection fraction; FS = fractional shortening; LV = left ventricular.

volumes within 1 min, reducing ejection fraction from 71.4 ± 9.2% to 38.7 ± 18.8%. In parallel, short-axis cross-sectional dimensions increased, decreasing short-axis area shortening from 67.0 ± 7.2% to 27.5 ± 20.7% (Table 1). After this initial period, left ventricular volumes gradually decreased, leading to a gradual increase in ejection fraction and short-axis area shortening, gaining significance ($p < 0.05$) 30 min after microembolization (ejection fraction 45.7 ± 14%; short-axis area shortening 44.2 ± 12%).

Heart rate, systolic left ventricular pressure and systolic and diastolic aortic pressures remained unchanged throughout the experiment (Table 1).

Effect of coronary microembolizations on regional wall motion. Microembolizations were performed in the left circumflex coronary artery in five animals and in the left anterior descending artery in one. Microembolization decreased segmental fractional area shortening within a period of 1 min. This decrease in regional function was most pronounced in the areas corresponding to the coronary artery flow bed.

After microembolization, mild to moderate hypokinesia (fractional area shortening >20%) developed in 45 segments, reducing fractional shortening from 64 ± 14% to 41 ± 13%. Severe hypokinesia (fractional area shortening ≤20%) developed in 20 segments, reducing fractional shortening from 60 ± 15% to 13 ± 5%. Akinesia developed in six segments, and dyskinesia in five. With dyskinesia, fractional shortening received negative values as expected, decreasing to −10 ± 8%.

Changes in wall motion score derived from visual inspection correlated only modestly ($r = 0.5$) with changes in segmental fractional area shortening (Fig. 2).

Regional wall motion assessed by phase and amplitude imaging. Visual inspection of the phase image showed uniform phase angles in areas relating to maximal endocardial inward motion at baseline. These phase angles were displayed in shades of green color (Fig. 1). During microembolization, focal areas were identified on the phase image with a color code indicating delayed endocardial motion (Fig. 3). In akinetic segments, indeterminate or undefined phase angles were identified by a characteristic "salt-and-pepper" appearance (Fig. 4). In dyskinetic segments, phase angle shifts were characterized by a shift in color of ~180°.

Figure 2. Correlation of visual assessment of wall motion with segmental fractional shortening. Δ = change.

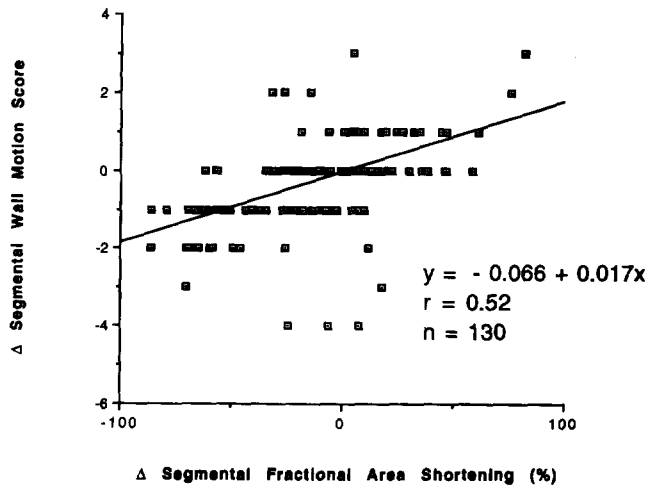

JACC Vol. 25, No. 6
May 1995:1436–44

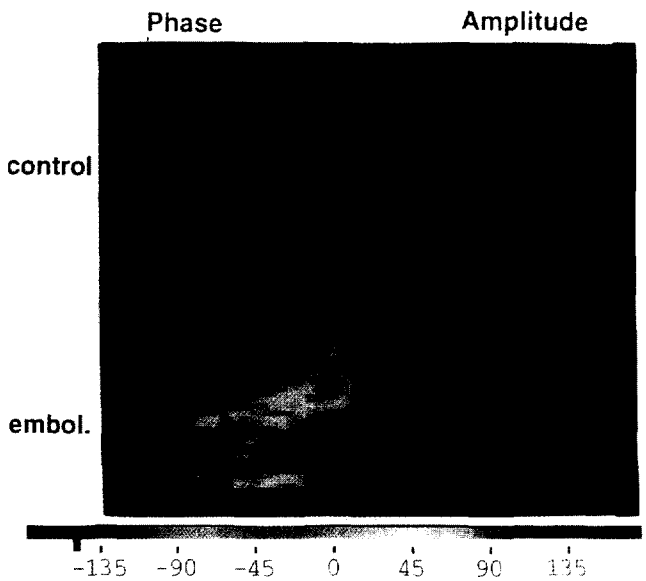

Figure 3. Changes in phase angles and amplitudes in a region of interest in a posterior wall segment. Magnified posterior wall segment shows synchronous phase angles (**left**) and uniform amplitudes (**right**) during baseline (control [**top**]). After microembolization (embol. [**bottom**]), amplitude was reduced, and phase angles were asynchronous, as indicated by altered **color codes**. Because different thresholds were used to increase signal/noise ratio, color codes between baseline and embolization periods are different. However, note the phase angle distribution within the posterior wall segment during embolization, indicating delayed endocardial motion in the basal portion of the wall segment (**blue color code**), whereas motion was less delayed in the remaining segment (**green color code**).

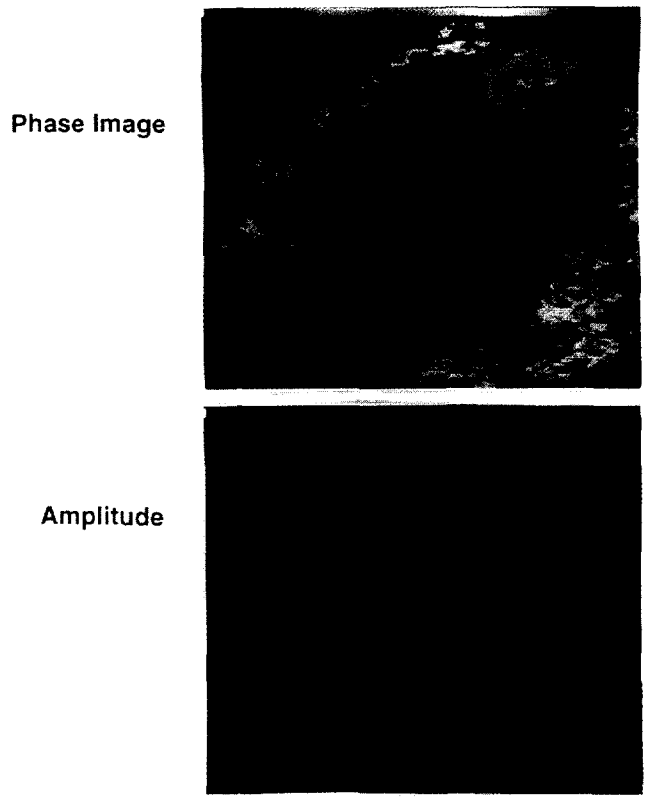

Figure 4. Phase (**top**) and amplitude images (**bottom**) of a long-axis view during microembolization-induced ischemia. Note absence of defined phase and amplitude values indicated by the "salt-and-pepper" appearance in the lateral wall segment. Note that in the basal portion of the septum (**black arrowheads**), amplitude is less, and phase angles are shifted to the left relative to normal motion in the remaining septal wall.

With decreasing segmental fractional shortening, phase angles were progressively delayed. In mild to moderate hypokinetic segments, relative phase angles increased significantly from 6 ± 10° to 47 ± 44° ($p < 0.05$). In severely hypokinetic segments, this delay increased further to 77 ± 63°. In akinetic segments phase angles were indeterminate, as indicated by the "salt-and-pepper" appearance of background noise. In dyskinetic segments phase angles were maximally delayed by 165 ± 17° ($p < 0.001$).

Directional changes in segmental fractional area shortening correlated well with directional shifts in phase angles (Fig. 5).

Normal endocardial motion yielded uniformly high amplitudes, with a mean segmental amplitude of 105 ± 30 gray level intensity. Hypokinesia resulted in low amplitudes, whereas akinesia resulted in a lack of regional amplitudes.

Amplitudes decreased with decreasing segmental fractional area shortening. In segments developing mild to moderate hypokinesia, amplitudes decreased from 80 ± 36 to 53 ± 34 gray level intensity. In segments developing severe hypokinesia, amplitudes decreased from 93 ± 36 to 45 ± 43 gray level intensity. In akinetic segments, amplitudes were absent because of the lack of endocardial motion and gray level changes. During dyskinesia amplitudes were decreased (35 ± 28 gray level intensity) in regions of outward endocardial motion.

Directional changes in segmental fractional area shortening correlated poorly with directional shifts in absolute amplitudes, but they correlated better with amplitudes normalized for ventricular size (Fig. 6).

Figure 5. Directional changes (Δ) in segmental fractional shortening compared with those in segmental phase angles.

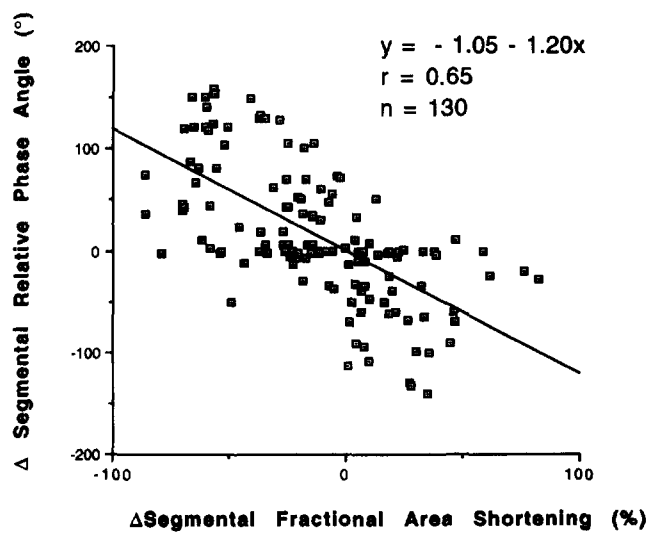

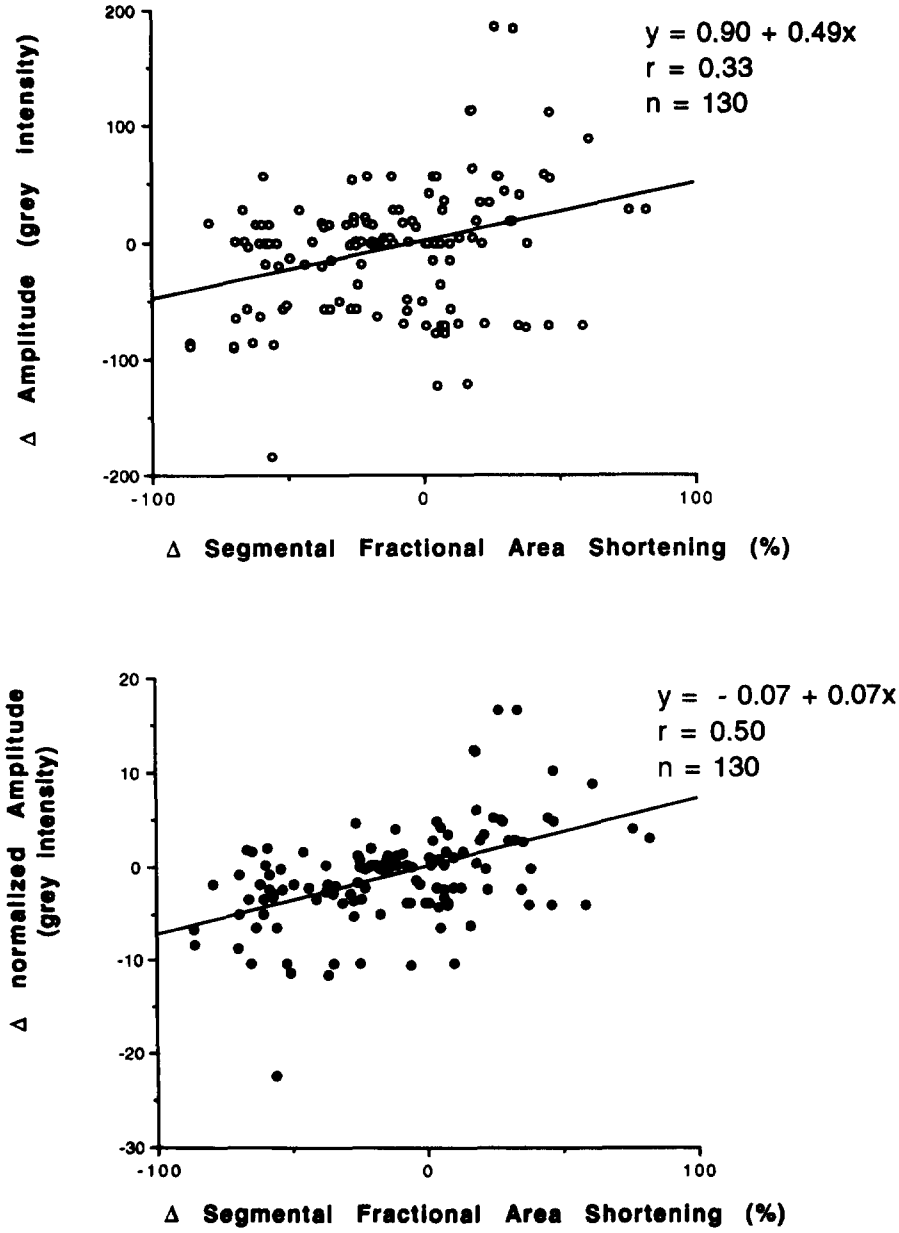

Figure 6. Amplitudes normalized for long axis correlated better with segmental fractional area shortening than did amplitudes not normalized. Δ = change.

In vitro model of temporal sequence of endocardial inward motion. Temporal shifts in the periodic motion of a phantom endocardial border were correctly indicated by shifts in phase angles (Fig. 7). Delays in endocardial motion by a single frame interval (33 ms) were indicated by a delay in phase angles of 36°, with 10 single frames comprising a complete cycle.

Comparison of phase angle shifts with temporal sequence of endocardial motion assessed by M-mode echocardiography in normal humans. Phase angle sequence derived from Fourier phase analysis of two-dimensional cine loops correctly identified the temporal sequence of wall motion derived from M-mode echocardiograms. Peak septal posterior motion occurred earlier than peak anterior motion of the posterior wall. Time to peak septal motion measured by M-mode echocardiography was significantly shorter than time to peak anterior motion of the posterior wall (time to peak septal motion 326 ± 28 ms vs. time to peak posterior wall motion 388 ± 26 ms, $p < 0.001$). This delay in peak posterior wall motion was indicated by a phase angle delay of 14.8 ± 2.2°.

Discussion

Phase and amplitude imaging for regional wall motion analysis. The results of our study demonstrate that Fourier phase and amplitude analysis of two-dimensional echocardiograms can be used to evaluate ischemia-related regional wall asynergy. Phase angles were delayed, and amplitudes were reduced, in ventricular segments with impaired wall motion

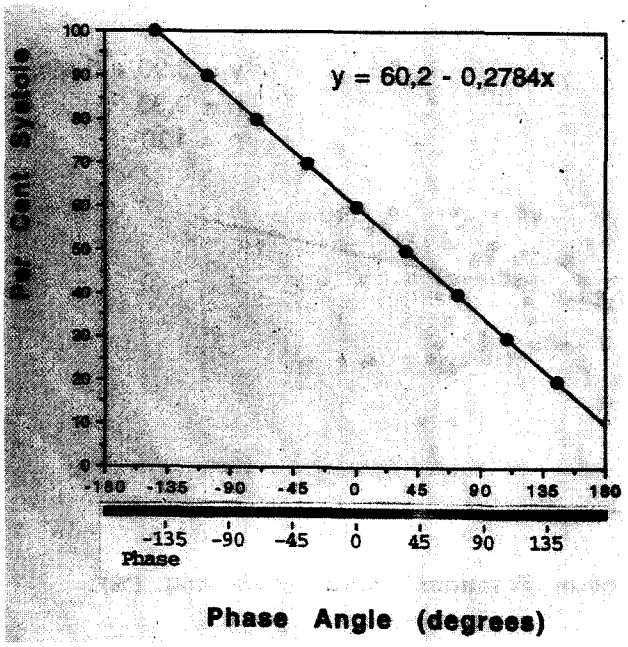

Figure 7. Relation between sequence of phase angles and relative duration of systole assessed in an in vitro model. With increasing duration of systole, phase angles shifted linearly to the left, indicating endocardial motion lagging behind normal motion.

induced by coronary microembolizations. The changes in phase angles correlated better with segmental fractional area shortening than did changes in amplitude and changes in wall motion scores. These findings are in accord with previous reports (14,16,17) using phase imaging of multigated acquisition equilibrium blood pool studies to evaluate regional wall motion.

Although they use the same mathematical Fourier transformation, phase analysis of two-dimensional echocardiograms is different from that of gated blood pool studies. Fourier phase analysis was first introduced as a method of evaluating the temporal sequence of ventricular wall motion by radionuclide ventriculography (1–4). The periodic nature of time–activity curves of the blood pool is submitted to temporal Fourier analysis. Fourier analysis is a mathematical method that expresses any periodic function as the sum of sine and cosine waves of different frequencies and amplitudes. Radionuclide phase imaging is based on a first-harmonic Fourier transformation of time–activity curves of pixels relating to the blood pool. The resulting phase and amplitude images are displayed as color-encoded images. In contrast to blood pool studies, phase and amplitude imaging applied to two-dimensional echocardiography is based on analysis of periodic endocardial motion. Phase analysis was first applied to two-dimensional echocardiography to characterize altered ventricular contraction sequence during right ventricular pacing and to localize accessory bypass tracts in patients with the Wolff–Parkinson–White syndrome (7).

In the present study, normal wall motion was characterized by uniform amplitudes and homogeneous phase angles, using both qualitative visual inspection and quantitative analysis of various wall segments. In contrast, phase analysis in normal human subjects showed nonuniform contraction with a progression in phase angle sequence from anteroseptal and left anterior segments to lateral segments with progression of phase delay to posterior segments, as reported previously (7). This sequence of mechanical activation is in accordance with the sequence of electrical activation found in isolated human hearts (18) and in in situ dog hearts (19). Nonuniform ventricular contraction has also been demonstrated in frame-by-frame analysis of angiographic studies measuring radial shortening (20,21) or hemiaxis shortening (22). Inward motion was earliest near the base of the heart and latest in the apical region, with lower amplitude at apical and midanterior segments. This nonuniformity of normal ventricular contraction is best explained by two factors: 1) Electrical activation sequence of the myocardium may lead to nonuniform mechanical activation; 2) myocardial fiber orientation may add to asynchronous wall motion. Whereas motion of anterior and inferior regions results from circumferentially oriented fibers, apical motion is caused by longitudinally directed fibers (9,23,24). By echocardiography, fractional area shortening, wall thickening and velocity of circumferential fiber shortening were shown to increase from base to apex as seen in cross-sectional views (25,26). This increased extent of shortening toward the apex of the ventricle was also found in experimental studies using ultrasound crystals (27). The finding that nonuniformity of normal wall motion was not detected by phase analysis in the present study is most likely explained by the limited resolution of the echocardiogram.

With decreasing segmental fractional shortening in areas developing wall motion abnormalities after coronary microembolization, phase angles were delayed, and amplitudes were reduced. This delay in segmental phase angles indicating marked asynchrony of myocardial contraction during ischemia is in accord with previous findings. It has been shown (9,10,12) that in patients with regional asynergy the time of systolic motion was significantly prolonged. Development of asynchrony during ischemia has also been demonstrated in isolated papillary muscle (11,28). Prolongation of time to peak tension and relaxation time have been suggested as possible factors explaining this asynergy associated with regional myocardial ischemia.

The use of phase analysis of gated blood pool images to quantitate regional wall motion abnormalities has been controversial. Some investigators (4,14) found a good correlation between the phase delay and the degree of contraction abnormalities. Mancini et al. (28) reported that radionuclide phase imaging is insensitive in characterizing wall motion abnormalities, especially when directional changes in wall motion are assessed. Echocardiographic phase imaging may have potential advantages over radionuclide phase imaging in assessing regional wall motion. In contrast to radionuclide phase imaging, echocardiographic phase imaging directly analyzes endocardial motion, whereas radionuclide imaging analyzes multigated blood pools, thus only indirectly deriving information on

regional wall motion. The concept of echocardiographic amplitude imaging in reference to a left ventricular wall differs from that of radionuclide imaging technique. In radionuclide imaging, amplitudes relate to intensity changes of the cardiac blood pool, whereas in echocardiographic imaging, amplitudes relate to the extent of wall motion (Fig. 4). In addition, radionuclide imaging is confined to finite time periods for image acquisition, whereas two-dimensional echocardiography has the ability to visualize cardiac motion on a beat-to-beat basis.

Potential advantages of echocardiographic phase and amplitude imaging. Echocardiographic Fourier phase and amplitude imaging may have potential advantages over conventional methods for assessing regional wall motion. Phase imaging visualizes the temporal sequence of endocardial motion encompassing a complete cine loop cycle, whereas calculation of segmental fractional area shortening analyzes segmental areas of end-diastolic and end-systolic frames only. Frame-by-frame analysis of computerized digital cine loop images may also provide information on periodic endocardial motion involving a complete cardiac cycle. However, frame-by-frame analysis is time-consuming and subjective, whereas the phase and amplitude images of a single cross-sectional view can be obtained and analyzed within 6 min and display endocardial motion in a more objective, simple format.

Potential limitations of echocardiographic phase and amplitude imaging. Several potential limitations of the present study must be considered. The mathematical transformation of echocardiographic images using a first-harmonic Fourier analysis algorithm may be limited because the curve fit to a cosine function may be only an approximation of the true time–pixel intensity curve. However, it is unlikely that the curve-fitting algorithm itself accounted for the phase angle shifts seen between wall segments.

Heart rate, by its influence on the relative duration of systole and diastole, may affect curve symmetry, which may influence the absolute timing of regional phase delay in normal patients (4). To overcome this limitation, we compared the regional phase angle in abnormally contracting segments with that in normally contracting segments within the same patient. We used this approach in our study so that the relative sequence of phase angles between various segments was unlikely to be affected by heart rate.

In addition, heart rate, by its effect on temporal resolution of digital cine loops, may significantly influence the sensitivity of the method. Increasing heart rate lowers the number of frames comprising a digital cine loop, decreasing temporal resolution and potentially lowering sensitivity of the method. In the present dog model mean heart rates were relatively high, ranging from 153 to 168 beats/min, so that the sensitivity of echocardiographic phase imaging improves when heart rate is slower because temporal resolution is enhanced.

A variable quality of echocardiographic images is another factor limiting the applicability of echocardiographic phase and amplitude imaging. Phase imaging applied to echocardiography depends on the presence of a clearly defined endocardial edge. In wall segments where clear visualization of the endocardium is not possible, meaningful phase angles and amplitudes, as a consequence, cannot be derived. In the present dog model, high resolution images of the heart could be obtained from the chest wall because of the close proximity of the transducer to cardiac structures. In humans, transthoracic imaging may not sufficiently visualize endocardial borders, and other imaging methods such as transesophageal echocardiography may be more useful.

Rotational and translational movements of the heart may also have influenced phase angle values (29,30) but are unlikely to account for the marked phase shifts found in focal areas during ischemia. To minimize the confounding influence of rotational and translational motions, wall motion analysis methods using floating reference systems have been proposed. However, some investigators (31) have reported that the fixed external reference system is optimal for the short-axis view at the papillary muscle level. We used a fixed external reference system to analyze segmental fractional area shortening to allow better comparison with phase and amplitude images because the Fourier algorithm does not correct for rotational or translational axis shifts when analyzing time–pixel intensity curves.

Other variables, such as right ventricular volume or pressure overload, and ventricular conduction abnormalities, such as left bundle branch block (32), may result in abnormal (paradoxic) septal motion, confounding phase and amplitude imaging. However, these conditions were not present in our study.

Finally, the temporal sequence of endocardial motion in dogs, as assessed by the sequence of phase angles, was not directly compared with an independent reference method, such as assessment of wall motion using implantable sonomicrometers. However, to address this problem, the temporal sequence of wall motion in humans was analyzed using M-mode echocardiography as an independent method for displaying endocardial wall motion with high resolution. The temporal sequence of wall motion determined by M-mode echocardiography showed good agreement with the phase angle sequence found in the same segments.

Clinical implications. Fourier phase and amplitude imaging may provide an objective method of evaluating regional wall motion. As shown in the present study, regional wall motion abnormalities developing during myocardial ischemia can be adequately detected and quantitated using phase imaging to demonstrate altered contraction sequence and amplitude imaging to demonstrate diminished endocardial motion. Phase and amplitude imaging has the potential for incorporation into imaging systems, thus facilitating rapid and objective assessment of regional wall motion.

References

1. Adam WE, Geffers H, Kampmann H, Bitter F, Stauch M. Regional myocardial motility as evaluated by analysis of "gated blood pool" data. Z Kardiol 1977;66:545–55.
2. Bacharach SL, Green MV, Bonow RO, et al. A method for objective evaluation of functional images. J Nucl Med 23;1982:285–90.

3. Links LM, Douglass KH, Wagner HN. Patterns of ventricular emptying by Fourier analysis of gated blood-pool studies. J Nucl Med 1980;21:978–82.
4. Botvinick E, Dunn R, Frais M, et al. The phase image: its relationship to patterns of contraction and conduction. Circulation 1982;65:551–60.
5. Lyons J, Norell M, Gardener J, Davies S, Balcon R, Layton C. Phase and amplitude analysis of exercise digital left ventriculograms in patients with coronary disease. Br Heart J 1989;62:102–11.
6. Lyons J, Norell M, Gardener J, Balcon R, Layton C. The demonstration of exercise induced myocardial ischemia using phase and amplitude analysis of exercise digital left ventriculograms. Eur Heart J 1987;8:137–41.
7. Kuecherer HF, Abbott JA, Botvinick EH, et al. Two-dimensional echocardiographic phase analysis: its potential for noninvasive localization of accessory pathways in patients with Wolff–Parkinson–White syndrome. Circulation 1992;85:130–42.
8. Herman MV, Heinle RA, Klein MD, Gorlin R. Localized disorders in myocardial contraction: asynergy and its role in congestive heart failure. N Engl J Med 1967;277:222–32.
9. Gibson D, Mehmel H, Schwarz F, Li K, Kübler W. Changes in left ventricular regional asynchrony after intracoronary thrombolysis in patients with impending myocardial infarction. Br Heart J 1986;56:121–30.
10. Holman BL, Wynne J, Idoine J, Neill J. Disruption in the temporal sequence of regional ventricular contraction. I. Characteristics and incidence in coronary artery disease. Circulation 1980;61:1075–83.
11. Tyberg JV, Parmley WW, Sonnenblick EH. In vitro studies of myocardial asynchrony and regional hypoxia. Circ Res 1969;25:569–79.
12. Gibson DG, Doran GH, Traill TA, Brown DJ. Abnormal left ventricular wall movement during early systole in patients with angina pectoris. Br Heart J 1978;40:758–66.
13. Sabbah HN, Stein PD, Kono T, et al. A canine model of chronic heart failure produced by multiple sequential coronary microembolizations. Am J Physiol 1991;260:H1379–84.
14. Schiller NB, Shah PM, Crawford M, et al. Recommendations for quantitation of the left ventricle by two-dimensional echocardiography. J Am Soc Echo 1989;2:358–67.
15. Moynihan PF, Parisi AF, Feldman CL. Quantitative detection of regional left ventricular contraction abnormalities by two-dimensional echocardiography. I. Analysis of methods. Circulation 1981;63:752–60.
16. Frais M, Botvinick EH, Shosa D, et al. Phase image characterization of localized and generalized left ventricular contraction abnormalities. J Am Coll Cardiol 1984;4:987–98.
17. Ratib O, Henze E, Schön H, Schelbert HR. Phase analysis of radionuclide ventriculograms for the detection of coronary artery disease. Am Heart J 1982;104:1–12.
18. Durrer D, van Dam T, Freud GE, Janse MJ, Meijler FC, Arzbaecher RC. Total excitation of the isolated human heart. Circulation 1970;41:899–912.
19. Hotta S. The sequence of mechanical activation of the ventricle. Jpn Circ J 1967;31:1568–72.
20. Hammermeister KE, Gibson DG, Hughes D. Regional variation in the timing and extent of left ventricular wall motion in normal subjects. Br Heart J 1986;56:226–35.
21. Klausner SC, Blair TJ, Bulawa WF, Jeppsen GM, Jensen RL, Clayton PD. Quantitative analysis of segmental wall motion through systole and diastole in the normal human left ventricle. Circulation 1982;65:580–90.
22. Clayton PD, Bulawa WF, Klausner SC, Urie PM, Marshall HW, Warner HR. The characteristic sequence for the onset of contraction in the normal human left ventricle. Circulation 1979;59:671–9.
23. Rushmer RF, Crystal DIC, Wagner C. The functional anatomy of ventricular contraction. Circ Res 1953;1:162–70.
24. Greenbaum RA, Ho SY, Gibson DG, Becker AE, Anderson RH. Left ventricular fiber architecture in man. Br Heart J 1981;45:248–63.
25. Haendchen RV, Wyatt HL, Maurer G, et al. Quantitation of regional cardiac function by two-dimensional echocardiography. I. Patterns of contraction in the normal left ventricle. Circulation 1983;67:1234–45.
26. Shapiro E, Marier DL, St John Sutton MG, Gibson DG. Regional nonuniformity of wall dynamics in normal left ventricle. Br Heart J 1981;45:264–70.
27. LeWinter MM, Kent RS, Kroener JM, Carew TE, Corell JW. Regional differences in myocardial performance in the left ventricle of the dog. Circ Res 1975;37:191–9.
28. Mancini GBJ, Peck WW, Slutsky RA, et al. Analysis of phase angle histograms from equilibrium radionuclide studies: correlation with semiquantitative grading of wall motion. Am J Cardiol 1985;55:535–40.
29. Lee VW, Getchell J, Foster JE, Salzman L, Plehn J. Rotational artifact in phase imaging of cardiac scans: potential pitfalls in diagnosis. J Nucl Med 1987;28:1536–9.
30. Arts T, Meerbaum S, Reneman RS, Corday E. Torsion of the left ventricle during the ejection phase in the intact dog. Cardiovasc Res 1984;8:183–93.
31. Scnitger I, Fitzgerald PJ, Gordon EP, Alderman EL, Popp RL. Computerized quantitative analysis of left ventricular wall motion by two-dimensional echocardiography. Circulation 1984;70:242–54.
32. McDonald IG. Echocardiographic demonstration of abnormal motion of the interventricular septum in left bundle branch block. Circulation 1973;48:272.